DOI: 10.61782/fa.2025.0405

FORUM ACUSTICUM
EURONOISE 2025

FLAT AND CURVED PARAMETRIC ACOUSTIC LOUDSPEAKERS MEASURED WITH EXPONENTIAL SINE SWEEPS

Augusto Fantinelli[1] **Marc Arnela**[1*]

[1] Human-Environment Research (HER) group, La Salle, Universitat Ramon Llull, Barcelona, Catalonia, Spain

ABSTRACT

Parametric Acoustic Loudspeakers (PALs) utilise ultrasounds to generate an audible field thanks to a non-linear effect in air. This phenomenon is difficult to simulate, so an alternative is to rely on prototyping devices and test them experimentally. Several options exist to manufacture a PAL, the flat surface being the most common. However, transducers can also be set on curved surfaces to attain specific effects. In this paper, a set of four prototypes with different transducer dispositions on flat and convex surfaces are constructed and tested in free-field conditions at several distances. A methodology based on the Exponential Sine Sweep is used for this aim, which allows us to obtain their ultrasonic and audible frequency responses simultaneously. The results were compared with those of a single transducer, revealing significant differences between flat and curved PALs attributed to constructive and destructive interference patterns that vary with transducer arrangement.

Keywords: *parametric acoustic loudspeakers, frequency response, ultrasonic and audible sound fields, exponential sine sweeps, spatial sound-field sampling*

1. INTRODUCTION

Parametric acoustic loudspeakers (PAL) are devices that generate audible sound using ultrasonic transducers [1, 2]. They rely on the Parametric Acoustic Array (PAA) effect, in which the propagation of two ultrasonic frequencies in a medium generates a secondary field that oscillates with the difference between the frequencies. This difference can be tuned to be audible, allowing these devices to reproduce audio focused through the ultrasonic beam, making them useful for a vast gamma of applications [3].

The PAA effect results from the non-linear behaviour of the propagation media at elevated frequencies, and the equations that describe this phenomenon tend to have elevated mathematical and computational complexity [2, 4–7]. This makes the numerical modelling of this type of device difficult. To circumvent the need for simulations, prototypes of PALs can be constructed at relatively low costs since the ultrasonic transducers are inexpensive and 3D printing is currently an accessible process. Notwithstanding, the differences in the sound fields generated by different prototype models still need to be assessed.

This paper presents a comparison between 4 different prototypes of PAL that differ in shape (flat or curved), size, and amount of transducers. Two of them are flat, with one laying 96 transducers in concentric rings up to a diameter of 195 mm [8], while the other has 19 of them in a compact hexagonal distribution with diameter 82 mm. The other two are curved, with one of them being an omnidirectional source with 750 transducers placed on a sphere of 250 mm of diameter [9], and the other being a spherical cap of 91 mm and 19 transducers with the same curvature than the omnidirectional source. Exponential Sine Sweeps (ESS) were adapted and employed to be used in these loudspeakers, allowing the simultaneous measurement of the frequency response in the audible and ultrasonic ranges [10, 11]. A robotic system was used to

*__Corresponding author__: marc.arnela@salle.url.edu.

place the transducer at increasing distances from 10 mm up to 2.13 m, and the frequency responses were taken at each point.

This paper is structured as follows. Section 2 presents the prototypes and the method used to measure the sound field they generate. Section 3 shows the results obtained for each prototype and presents considerations regarding their differences. Section 4 closes the paper with the conclusions.

2. METHODOLOGY

2.1 Exponential Sine Sweep methodology applied to PAL

An Exponential Sine Sweep (ESS) can be defined as [10]

$$s(t) = K \sin\left[K\ (\exp(t/L) - 1)\right], \tag{1a}$$

in which

$$K = \frac{2\pi f_1 T}{\ln(f_2/f_1)}, \tag{1b}$$

$$L = \frac{T}{\ln(f_2/f_1)}, \tag{1c}$$

and f_1 and f_2 are the lower and upper frequencies of the sweep, respectively. This represents a sine function of amplitude K in which the argument exponentially increases in time. This sweep is played through a loudspeaker inside an enclosure and recorded by a microphone. The deconvolution of the recorded signal through an inverse filter corresponding to the sweep results in an impulse response that contains information about the speaker, room and microphone. This technique has been vastly used in acoustics due to its robustness to noise and distortion [12–14].

The utilisation of ESSs in PALs [10, 11] requires the sweep to be modulated into a frequency range appropriate to the ultrasonic transducers that form the PAL. The signals, therefore, go through an upper side-band amplitude modulation (USBAM) with a transmitted carrier component. This, in practice, means that the transducers are constantly emitting the transmitted carrier with frequency f_c and whatever the frequency of the sweep signal at that moment. The simultaneous emission of both frequencies triggers the PAA effect. This allows for the frequency responses in the audible and ultrasonic ranges to be measured simultaneously [10, 11].

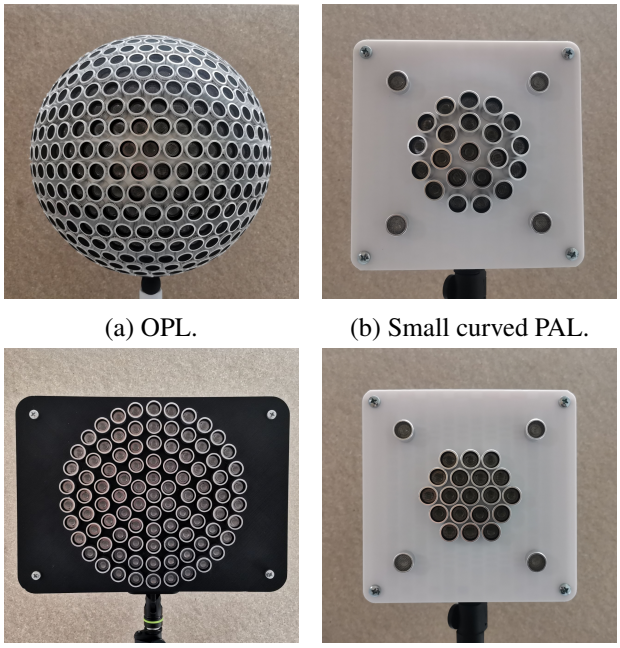

(a) OPL. (b) Small curved PAL.

(c) Flat PAL. (d) Small flat PAL.

Figure 1: PALs analysed in this work.

2.2 Prototypes

Four prototypes of PAL are considered. They all employ the same transducer model (Multicomp Pro MCUST16A40S12RO), varying in quantity and/or disposition. These transducers are ultrasonic piezoelectric transducers (PZTs) and are connected in parallel in all models. Figure 1 displays the four parametric loudspeakers analysed in this work. The Omnidirectional Parametric Loudspeaker (OPL) was designed and constructed in [9], characterised in [10, 11] and applied in [15] for measuring the random-incidence sound absorption. It has 750 transducers arranged in a sphere with 250 mm of diameter following an equal-area distribution [9]. The OPL directly inspires the next prototype. It is based on its top spherical cap, with 91 mm of diameter and 21 transducers. Next is the flat PAL described in [8], with 96 transducers laid out in six circular rings up to 195 mm of diameter. The last prototype has its transducers set in a hexagonal manner, with three layers and 19 transducers, and has 82 mm of diameter. In addition to the PALs, the same transducer that composed all prototypes was also analysed.

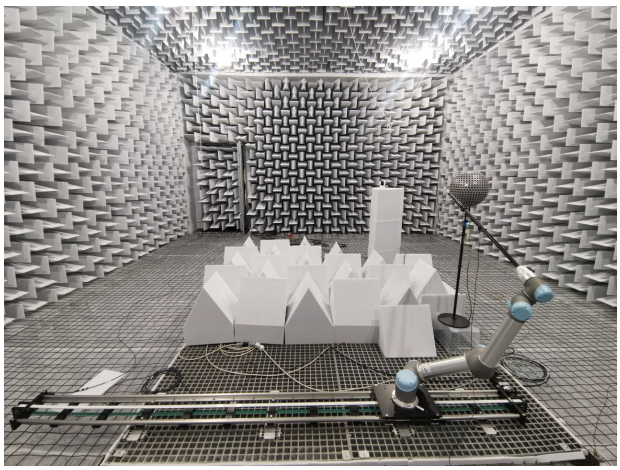

Figure 2: Experimental setup in the anechoic chamber of La Salle - Universitat Ramon Llull, with the robot, the track and the OPL installed.

2.3 Experimental setup

A UR5 (Universal Robots) robotic arm was used to position the microphone aligned with the centre of the irradiation. The robot is mounted over a $2.45\,\mathrm{m}$ linear track (IGUS) so it can be moved around parallel to the x axis of the speaker. The sound field emitted by the prototypes was measured along the centre of the propagation axis for all loudspeakers (aligned with the movement axis of the track) with an interval of $0.04\,\mathrm{m}$, from $0.01\,\mathrm{m}$ to $2.13\,\mathrm{m}$ of distance from the closest transducer. A GRAS 46BF-1 1/4" microphone was attached to the robot by a $1\,\mathrm{m}$ microphone holder, long enough so the robot causes minimal effects in the measured sound field. The generation of the sine sweep and the recordings were made using a Type 3160-A-042 Brüel & Kjaer LANXI module with a UA-3102-041 front end. The signal was amplified using an Ecler XPA3000 amplifier with its gain set in such a way that it provides a peak voltage of $17\,\mathrm{V}$ to avoid damaging the transducers. Fig. 2 displays the experimental setup with the UR5 cobot and the Igus track used to scan the sound field generated by the OPL [9], assembled in the anechoic chamber at La Salle - Universitat Ramon Llull.

The ESSs emitted by the PALs were $1\,\mathrm{s}$ long, from $20\,\mathrm{Hz}$ to $14\,\mathrm{kHz}$, with $2\,\mathrm{s}$ and $3\,\mathrm{s}$ of silence before and after the sweep, respectively. Linear ramps from $20\,\mathrm{Hz}$ to $80\,\mathrm{Hz}$ and $12\,\mathrm{kHz}$to $14\,\mathrm{kHz}$ were added to the sweeps to avoid pre-ringing artefacts, as proposed in [10]. Due to the changes in impedance from one prototype to another and the response of the amplifier, an equalization of the sweep was done to compensate for the change in waveform and maintain the excitation voltage constant [15]. This is specifically important when employing the OPL due to its very capacitive load [15]. In addition, a $1\,\mathrm{kHz}$ modulated pure tone was measured to calibrate the measurement chain. This pure tone was measured at the central position of the array $10\,\mathrm{mm}$ from the loudspeaker. The ESSs were modulated using USBAM with carrier frequency $f_c = 41.4\,\mathrm{kHz}$, selected based on [10]. The same carrier frequency was used for all devices.

3. RESULTS AND DISCUSSIONS

Fig. 3 shows the frequency responses in front of the four PALs and the single PZT transducer for four different distances in the audible and ultrasonic frequency ranges. The first thing of note is that the audible frequency responses have shapes that follow the ultrasonic ones. This is especially noticeable when comparing the frequency responses between the two ranges close to the source, where the highest sound pressure levels (SPLs) occur. It can also be seen that very close to the source, the curved designs produce higher levels than the flat prototypes, except at about $54\,\mathrm{kHz}$, which is the second resonance of this transducer [16]. Note also that they produce the highest levels at low frequencies. This is likely related to the constructive and destructive interaction of the sound waves generated by the arrays, which is modified depending on whether the prototype is flat or curved. With increasing distance, the only PALs that generate over $60\,\mathrm{dB}$ are the flat PAL and the OPL, which have more transducers than the rest. The small flat PAL does not reach large distances compared to other prototypes. This indicates that the constructive and destructive interactions between the individual transducers influence the behaviour of the PAL, and the final resulting emission cannot be estimated with only the amount and the shape of the distribution. As expected, the single transducer also does not generate high level audible sound fields due to insufficient ultrasonic power in the far-field to trigger the PAA.

Fig. 4 displays the generated audible and ultrasonic SPLs along a straight line following the propagation axis in front of the PALs, for $500\,\mathrm{Hz}$, $1000\,\mathrm{Hz}$, $5000\,\mathrm{Hz}$, and $10\,000\,\mathrm{Hz}$. The sound field cast by a PAL can be divided into three zones regarding the distance: a near-field in which there are successive local minima and maxima of

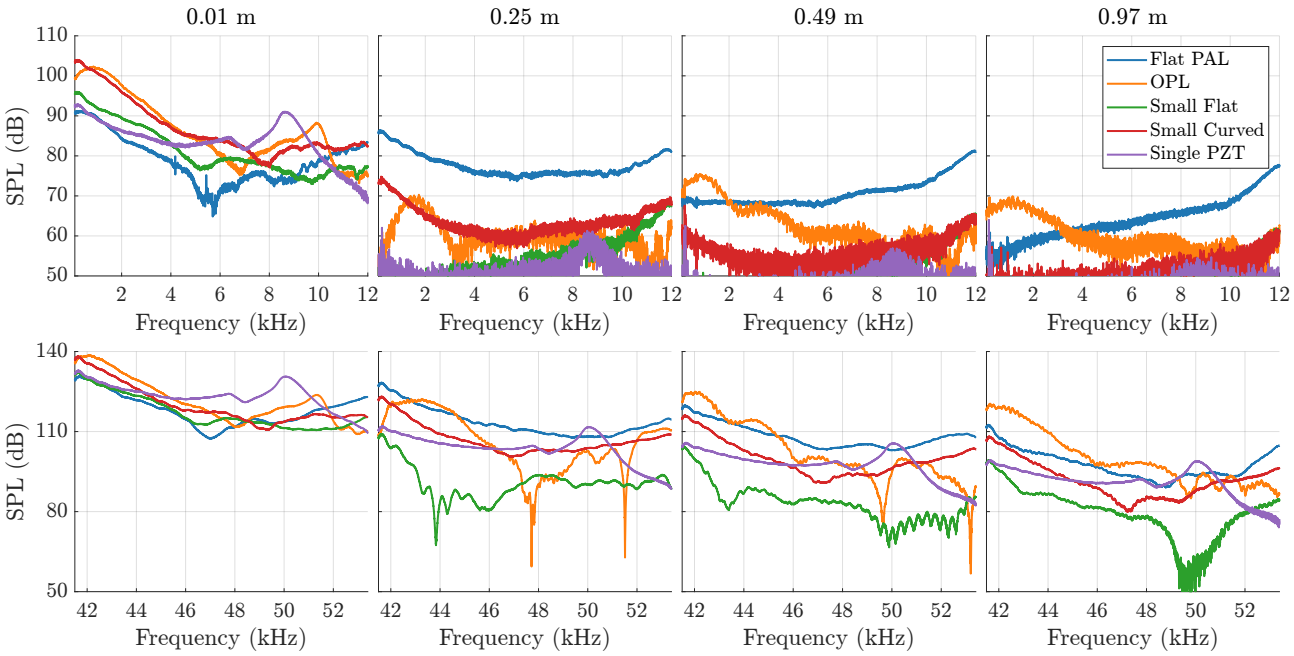

Figure 3: Frequency responses for the four PALs and the single transducer.

sound pressure; the Westervelt far-field, in which the PAL behaves like an infinitely large virtual volume source; and the inverse-law field, in which the inverse-square-law is valid [2]. The inverse-law field typically exists very far from the source, exceeding the dimensions of the anechoic chamber. Therefore, it was not assessed. The transition between near-field and Westervelt far-field can be identified following the criterion introduced by Zhong *et al.* [2]. This transition can be determined by finding the last local maxima of the SPL in the distance. The Westervelt far-field transition distances for the flat circular PAL (F. C. PAL), the flat hexagonal PAL (F. H. PAL), the OPL, and the spherical cap PAL (S. C. PAL) are displayed in Tab. 1. The small flat PAL and the single transducer do not produce high audible SPLs beyond the near-field, likely due to destructive interferences in the former and lack of power in the latter. Another thing of notice is that the flat PAL has a pronounced peak around the transition distance at 500 Hz, 1 kHz, and 5 kHz. Relating with Zhong *et al.*'s analysis [17], this indicates that this corresponds to a region where the sound energy is focused. At 10 kHz, the peak is not as pronounced, and the levels are higher in the Westervelt far-field, indicating the formation of a sound beam despite an initial concentration of energy.

Table 1: Westervelt far-field transition distance (m) at 500 Hz, 1 kHz, 5 kHz and 10 kHz for the flat PAL, the small flat PAL, the OPL, and the small curved PAL prototypes.

	500 Hz	1 kHz	5 kHz	10 kHz
Flat PAL	0.25 m	0.25 m	0.25 m	0.29 m
Small Flat	0.17 m	0.13 m	0.17 m	0.13 m
OPL	0.41 m	0.45 m	0.33 m	0.37 m
Small Curved	0.09 m	0.09 m	0.09 m	0.13 m

Regarding the ultrasonic field generated along the propagation axis (see Fig. 4), observe that the local maxima in the ultrasonic range coincide with the local maxima at the audible range. This indicates that the ultrasonic fields could also be used to determine the transition between near-field and Westerwelt far-field. Another remark is that the ultrasonic levels for the small flat PAL are very low, even lower than the single transducer. This means that, despite this PAL having 19 transducers, their ultrasonic signals suffer destructive interferences, and the generated levels are even lower than for the single transducer. Transducer placement and phase mismatch might be the causes of this phenomenon.

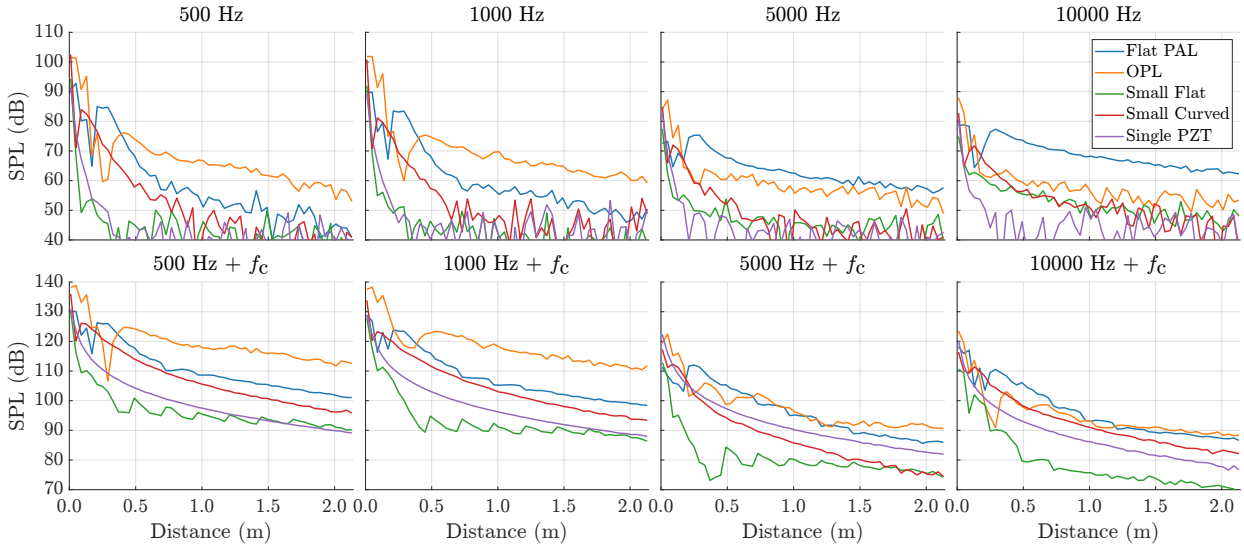

Figure 4: Audible (top) and ultrasonic (bottom) sound pressure levels (SPLs) for each device as a function of the distance from the speaker. $f_c = 41.4$ kHz.

4. CONCLUSIONS

This work has explored the performance of four prototypes of PAL with distinct characteristics: a flat circular PAL (flat PAL), a flat hexagonal PAL (small flat), an omnidirectional PAL (OPL), and a spherical cap PAL (small curved), aiming to assess differences between flat and curved layouts. Their audible and ultrasonic frequency responses were simultaneously measured in free-field conditions using exponential sine sweeps, as well as that of the transducer used to build the arrays. Their behaviour was examined at several distances aligned to their centres employing a robotic system that moved and positioned a microphone.

Results show that the audible and the ultrasonic frequency responses match each other in shape, indicating proportionality between the primary (ultrasonic) and secondary (audible) fields. The curved designs produced higher levels in the near field and reached longer distances compared to the flat prototypes for low and mid frequencies (< 2 kHz), while the flat prototypes have the opposite behaviour and generate the highest values at high frequencies. The flat PAL has a focusing behaviour in lower frequencies, in which the sound energy is concentrated in the transition region of the PAL. The prototypes with curved designs did not present this behaviour and, instead, tended to carry part of the sound energy throughout the distance, although with a pronounced decay at higher frequencies, while retaining part of the energy in the near-field. The small flat PAL generated very low ultrasonic levels in the far-field, which were not enough to trigger the PAA effect. All in all, the above behaviours could be justified by the constructive and destructive interaction of the ultrasonic sound fields generated by each of the transducers that form the array. It seems clear that modifying the number of transducers and their arrangement in the array, whether curved or flat, greatly affects the behaviour of the PAL.

Future work will involve applying near-field acoustical holography (NAH) to these and other prototypes and transducers to investigate the mechanisms of ultrasonic and audible sound generation, as well as the interactions among individual transducers. Their sound fields will also be analysed using pressure maps obtained with the assistance of a robotic measurement system.

5. ACKNOWLEDGMENTS

This work has been funded by MCIN/AEI/10.13039/501100011033 and the European Union - NextGenerationEU through project Sonora (TED2021-132376A-I00). The authors thank the support of the Catalan Government (Departament de Recerca i Universitats) for the grant 2021 SGR 01396 given to the HER group.

6. REFERENCES

[1] F. J. J. Pompei, *Sound from ultrasound*. PhD thesis, Massachusetts Institute of Technology, 2002.

[2] J. Zhong, R. Kirby, and X. Qiu, "The near field, westervelt far field, and inverse-law far field of the audio sound generated by parametric array loudspeakers," *J. Acoust. Soc. Am.*, vol. 149, no. 3, pp. 1524–1535, 2021.

[3] Holosonics, "Audio spotlight directional speakers." `https://www.holosonics.com/applications`. Last accessed 2025-04-07.

[4] O. Guasch and P. Sánchez-Martín, "Far-field directivity of parametric loudspeaker arrays set on curved surfaces," *Appl. Math. Model.*, vol. 60, pp. 721–738, 2018.

[5] J. Zhong, S. Wang, R. Kirby, and X. Qiu, "Insertion loss of a thin partition for audio sounds generated by a parametric array loudspeaker," *J. Acoust. Soc. Am.*, vol. 148, no. 1, pp. 226–235, 2020.

[6] J. Zhong, S. Wang, R. Kirby, and X. Qiu, "Reflection of audio sounds generated by a parametric array loudspeaker," *J. Acoust. Soc. Am.*, vol. 148, no. 4, pp. 2327–2336, 2020.

[7] J. Zhong, R. Kirby, M. Karimi, H. Zou, and X. Qiu, "Scattering by a rigid sphere of audio sound generated by a parametric array loudspeaker," *The Journal of the Acoustical Society of America*, vol. 151, pp. 1615–1626, 03 2022.

[8] M. Avelar, M. Arnela, C. Martínez-Suquía, L. Sant'Ana, and E. Brandão, "Medicão de coeficiente de espalhamento sonoro (scattering) em câmara anecoica, com auxílio de fontes sonoras paramétricas," in *XIII Iberoamerican Congress of Acoustics*, (Santiago, Chile), Iberoamerican Acoustics Federation, 2024.

[9] M. Arnela, O. Guasch, P. Sánchez-Martín, J. Camps, R. M. Alsina-Pagès, and C. Martínez-Suquía, "Construction of an omnidirectional parametric loudspeaker consisting in a spherical distribution of ultrasound transducers," *Sensors*, vol. 18, no. 12, p. 4317, 2018.

[10] M. Arnela, C. Martínez-Suquía, and O. Guasch, "Characterization of an omnidirectional parametric loudspeaker with exponential sine sweeps," *Appl. Acoust.*, vol. 182, p. 108268, 2021.

[11] M. Arnela, C. Martínez-Suquía, and O. Guasch, "Carrier frequency influence on the audible and ultrasonic fields generated by an omnidirectional parametric loudspeaker excited with exponential sine sweeps," *Appl. Acoust.*, vol. 200, p. 109073, 2022.

[12] A. Farina, "Simultaneous measurement of impulse response and distortion with a swept-sine technique," in *Audio Engineering Society Convention 108*, (Paris, France), pp. 1–24, Audio Engineering Society, 2000.

[13] S. Müller and P. Massarani, "Transfer-function measurement with sweeps," *Journal of the Audio Engineering Society*, vol. 49, pp. 443–471, 2001.

[14] A. Farina, "Advancements in impulse response measurements by sine sweeps," in *Audio Engineering Society Convention 122*, (Vienna, Austria), pp. 1–21, Audio Engineering Society, 2007.

[15] M. Arnela, R. Burbano-Escolà, R. Scoczynski Ribeiro, and O. Guasch, "Reverberation time and random-incidence sound absorption measured in the audible and ultrasonic ranges with an omnidirectional parametric loudspeaker," *Applied Acoustics*, vol. 229, p. 110414, 2025.

[16] A. Fantinelli, M. Arnela, R. Burbano-Escolà, and J. Vaquerizo-Serrano, "A study of the ultrasonic and audible frequency response of commercial loudspeakers for use as parametric acoustic arrays," in *Inter-noise 2024*, (Nantes, France), International Institute of Noise Control Engineering, 2024.

[17] J. Zhong, T. Zhuang, R. Kirby, M. Karimi, X. Qiu, H. Zou, and J. Lu, "Low frequency audio sound field generated by a focusing parametric array loudspeaker," *IEEE/ACM Transactions on Audio, Speech, and Language Processing*, vol. 30, pp. 3098–3108, 2022.